The Jominy End Quench for Light-Weight Alloy Development

J.W. Newkirk and D.S. MacKenzie

(Submitted 2 December 1999; in revised form 22 March 2000)

The Jominy end quench test is well known as a method of measuring hardenability in steels. In nonferrous alloys, there is a desire to determine the effect of quenching on final properties after heat treating. The Jominy end quench test offers a method for studying many quenching conditions with a minimum of samples. The potential for developing a new understanding of the complex response of nonferrous alloys to processing conditions, especially quenching, will be presented. Examples of the properties measured on Jominy end quench specimens of aluminum and titanium alloys will be presented.

Keywords aging, aluminum alloys, heat treatment, Jominy, quenching

1. Literature Review

In this section, a brief review of the available literature on the use of the Jominy end quench test will be described. The previous use of the Jominy end quench test for nonferrous alloys will be discussed, and the specific use of the Jominy end quench test for aluminum alloys will be shown.

2. Jominy End Quench

In the original classic work by Jominy and Boegehold,[1] they described a cylindrical specimen 100 mm long by 25 mm in diameter. The specimen was austenitized and then removed from the furnace and placed in a fixture, where the specimen was exposed at one end to a specified vertical stream of water. The resulting cooling is one dimensional and is invariant on the composition of the steel. But the resulting hardenability of the steel, as measured by hardness, is dependent on the composition and grain size of the steel. The simple design of the specimen, and the relative ease of the test procedure, has made this test the preferred method to measure the hardenability of steel. The popularity and repeatability of the test has resulted in the test procedure being adopted in ASTM,[2] SAE,[3] and other agencies' test methods. A schematic of the method is shown in Fig. 1.

Jominy[4] also described a test specimen with a slightly different configuration that was designed for shallow hardening steels. It provided for much faster cooling rates. This specimen was called the "type L specimen" and had a conical section removed from the quenched end to a depth of approximately 25 mm. The quenching conditions were changed slightly, requiring a free unimpeded water rise of 100 mm. Because of difficulties in machining and the sensitivity to small dimensional changes, this geometry was never adopted as a standard test method.

Hergat[5] described precautions that should be taken to achieve a 1 HRC precision when conducting the test. These improvements include making sure that the machined flats on the specimen are parallel and that the operator error induced during hardness testing is reduced by the use of semiautomatic hardness machines. It is also necessary to ensure that the specimen is in a fixture that ensures accurate positioning and firmly holds the specimen. It was found that the Vickers hardness test provided much better repeatability. Brown[6] also found that Vickers hardness measurements provided much better repeatability and allowed for more data to be taken because the indentations could be spaced much closer together, improving the signal-to-noise ratio. It was found that the precision of the test was also improved by the use of a calibrated positioning device that held the specimen firmly in place. One of the advantages cited for the use of Vickers hardness is that the measurements can be readily rechecked by measuring the diagonals again or by placing an additional indention alongside the disputed reading. He found that the repeatability of the standard Rockwell-type test was typically 2 HRC. Using a 15 kg load, he found that the variability of the hardness measured by Vickers was roughly half that of the Rockwell test. In his concluding comments, he indicated that accurately determined hardenability curves often show that the test introduces the scatter rather than does the steel.

The nature of the hardness distribution at specific distances in the Jominy end quench test was investigated by Sheikh.[7] Three different steels were examined, with the intent of understanding the scatter that occurs when testing. Probability plots were created from the hardness data on the three steels and interpreted. It was determined that the hardness scatter at each location on the Jominy end quench is normally distributed and therefore would be bounded by a 3-sigma around the mean. The expected probability distribution can be used to predict and establish upper and lower control limits for heat treatment.

Kura and Lorig[8,9] measured cooling rates as a function of austenitizing temperature, quenchant temperature, composition, and plate thickness. They described higher quench rates at the quenched end of the test bar than that of Jominy. This is probably due to the age of the instrumentation. Several cooling curves

J.W. Newkirk and **D.S. MacKenzie**, University of Missouri - Rolla. Rolla, MO 65409.

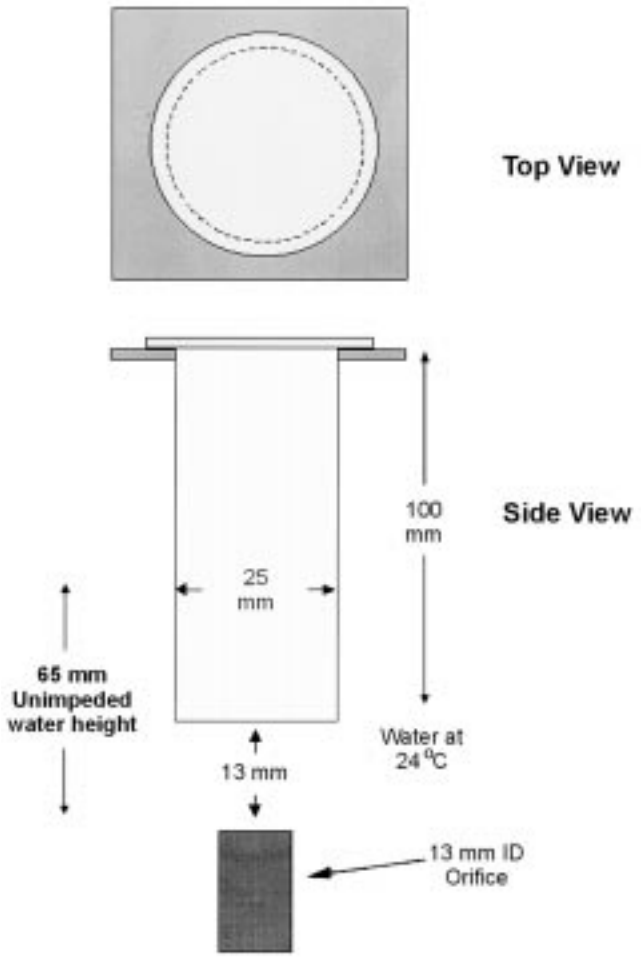

Fig. 1 Schematic of the Jominy end quench

are provided. Plates from 12.5 to 100 mm thick were examined. The severity of quench using Grossman quench factors was estimated for water and oil and correlated to plate thickness for the Jominy end quench test conditions. It was determined that the hardness within the cross section of a plate closely approximates that measured by the Jominy end quench test at equivalent cooling rates. This is applicable regardless of the quenchant or thickness of the plate, since it is a function of cooling rate.

3. Jominy End Quench of Nonferrous Alloys

There has been some published work on the use of the Jominy end quench test for nonferrous alloys. Toda[10] measured the critical cooling rates for Cu-Cr, Cu-Be, and Cu-Co_2Si using the Jominy end quench method. The cooling rates of these tests were determined using a pen-recording oscilloscope. It was determined that the critical cooling rate for the alloys investigated was the cooling rate that caused a decrease in properties. It was defined as the cooling rate necessary to obtain a supersaturated solid solution at room temperature. Both as-quenched and aged hardnesses were taken. In a study sponsored by Rolls Royce Aerospace, Postans[11] investigated the use of the Jominy end quench test for titanium alloys. He was able to use this technique successfully to establish the best alloy and quench rate for specific applications. He showed schematically how the microstructure of various titanium alloys varied as a function of cooling rate.

4. Jominy End Quench—Aluminum Alloys

There has been limited published work on the use of the Jominy end quench test for aluminum alloys. Loring *et al.*[12] authored the first published paper on the use of the Jominy end quench test for studying aluminum alloys using a modified L-type Jominy specimen. The cooling curves at various distances up to 25 mm were measured. Different types of aluminum (14S, 24S, 61S, R-301, and 75S) were tested. Hardnesses were measured at 3 mm intervals using the Rockwell B, F, and Vickers (5 kg) scales. Further, it was seen that higher quench rates yielded decreasing hardness in the as-quenched condition. Low cooling rates produced relatively small changes in the hardness. Only 75ST exhibited a sensitivity to quench rate after aging.

In the work by 'tHart *et al.*,[13] the Jominy end quench test was applied to extruded rods of 2024 and 7075. The bars were aged to the 2024-T4, 2024-T6, and 7075-T73 conditions. The Jominy bars were evaluated by transmission electron microscopy (TEM) and corrosion testing to examine the relationship between quench rate, corrosion properties, and microstructure. The cooling rate of Jominy specimens fabricated from 2024 and 7075 were measured. Vickers hardnesses were taken at 5 mm intervals. It was found that 7075 was strongly quench sensitive and that hardness increases were only found in the first 60 mm of the bar. It was found that the quench rate and tempering operation influenced the widths of the precipitate free zone (PFZ). With only two data points, it was shown that faster cooling rates made for thinner PFZ.

The authors also evaluated 7010 and P/M 7091 aluminum alloys heat treated to the T6 and T73 tempers.[14] Corrosion properties and microstructure were determined as a function of cooling rate. It was found that 7010 was quite quench-insensitive compared to 7075. It was found that the alloys were insensitive to SCC and EXCO. No effect related to quench rate was found. It was also observed that the PFZs in 7091 and 7075 were more dependent on quench rate than that of 7010.

Using an apparatus similar to a Jominy end quench, Hecker[15] evaluated aging cycles as a function of time for an Al-Mg-Si alloy. It was shown that silicon has a marked effect on the age hardening of Al-Zn-Mg-Cu aluminum alloys.

Alternative methods of end quenching, similar in principal to the Jominy end quench, have been tried. Bomas[16] determined the time-temperature-property diagram of an Al-Zn-Mg alloy. This was accomplished using a rectangular specimen 15 $\times$ 140 $\times$ 300 mm, with the 15 $\times$ 140 mm face of the specimen exposed to the quenchant stream. This enables the specimen to be exposed to one-dimensional heat transfer, in the same fashion as the Jominy end quench test. Tensile specimens were laid out perpendicular to the axis of the quench medium and enabled to be taken as a function of cooling rate during quench. Arthur *et al.*,[17] used an apparatus similar to Bomas to develop

Table 1 Elemental chemistry of purchased 7075 and 7050 extruded rounds

Specimen	Elemental chemistry (wt.%)									
	Cu	Fe	Si	Mn	Mg	Zn	Ni	Cr	Ti	Zr
7075-T6	1.36	0.20	0.10	0.04	2.62	5.77	0.003	0.20	0.0170	0.0115
7050-T7451	2.11	0.12	0.050	0.04	1.98	5.74	<0.000	0.026	0.031	0.09

models on the development of residual stresses during quenching in several aluminum alloys. He developed several constitutive equations used for modeling the heat transfer and mechanical properties at elevated temperatures. To determine the thermal conductivity, since it was unavailable for the temperatures of interest, an estimate of the thermal conductivity was made by fitting the thermal conductivity equation to the cooling curves. This is not a rigorous method but was adequate for their purposes.

Using an end quench apparatus similar to Arthur, Becker *et al.*,[18] presented very detailed constitutive models for Al-5.6% Mg alloy and pure aluminum. Models, as a function of temperature, included density, heat capacity thermal conductivity, thermal expansion, and mechanical properties. These models also provided the basic activation energies and other information for the temperature compensated strain rate (Z).

5. Experimental Procedure

The use of the Jominy end quench on a titanium alloy (Ti-6V-4Al) and two aluminum alloys (7075 and 7050) was accomplished. This was accomplished by validating the basic technique and examining whether radial heat transfer occurred. Once the basic technique had been validated, then hardness measurements and microstructure examination of the Ti-6V-4Al and aluminum alloys could be performed.

6. Raw Material

A length of 7075-T6 (37 mm diameter) and a length of 7050-T7451 (75 mm diameter) extruded rods were purchased for initial testing. The elemental chemistry of each of the extruded rods was verified using induction coupled argon plasma spectroscopy and compared to traceable standards. The results of the elemental chemistry are shown in Table 1. The material was examined for hardness and conductivity to verify the heat treated condition supplied. It was found that the hardness and conductivity of the 7075 and 7050 extruded rounds were typical of published values.

A 72 mm diameter rod of Ti-6V-4Al was obtained and examined for microstructure. The microstructure was found to be consistent with annealed Ti-6V-4Al. Vendor certificates of conformance were used for elemental chemistry.

7. Conducting the Jominy End Quench Test

From each of the materials, jominy end quench specimens were prepared per ASTM A255. The size of the extrusions and the smaller size of the jominy end quench specimens eliminated the narrow recrystallization layer at the surface of the aluminum extrusions. Any evidence of alpha-case on the titanium was also machined away. After machining, the specimens were cleaned in acetone to remove any trace of cutting fluids or hand oils.

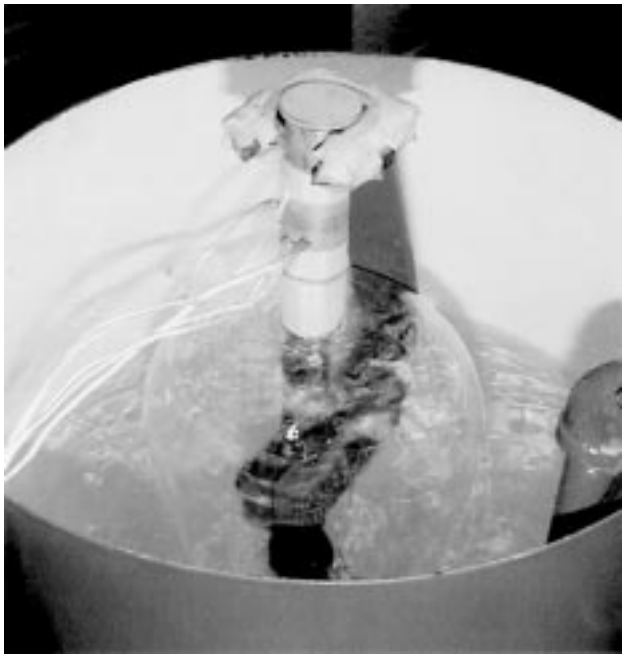

Fig. 2 Jominy end quench fixture used

The aluminum jominy end quench specimens were placed inside the furnace and heat treated for 1 h at 471 °C. The titanium specimens were heat treated for 1 h at 900 °C. While the test specimens were reaching the desired temperature, the setup of the Jominy end quench fixture was verified. The height fixture used is shown in Fig. 2.

Once the specimens had soaked at temperature, the furnace door was opened and the specimens were grabbed one at a time using either tongs or insulated gloved hands. The specimens were placed on the Jominy fixture and the water flow to the nozzle was initiated. The time elapsed between the time the door was opened and the time the water flow was initiated was approximately 5 s. The temperature drop of the furnace during specimen removal was about 4 °C. The specimen was allowed to cool for approximately 5 min. Once the temperature of the specimen was below 60 °C, then the specimen was removed from the fixture. The aluminum specimens were immediately placed in a chilled methanol bath at a temperature of −50 °C. This was done to control the time prior to aging. The titanium

specimens were allowed to cool to room temperature. No subsequent aging was performed on the titanium specimens.

After allowing the aluminum specimens to reach the equilibrium temperature of the methanol bath, the aluminum specimens were removed and placed in a room temperature water bath. After warming to room temperature, the samples were dried, and the specimens were allowed to sit at room temperature for 120 h. Once this time had elapsed, the specimens were placed again in the chilled methanol bath to end the natural aging cycle. This was done to ensure that no additional natural aging occurred prior to placing the specimens in the aging oven.

After reaching the equilibrium temperature of the bath, each aluminum specimen was removed from the methanol bath and placed in room temperature water. Once room temperature had been reached, the specimens were placed into the recirculating air aging furnace. Using a programmable temperature controller, the age cycle for each specimen was established and started. The aging cycle consisted of a first stage age at 108 °C for 5 h, followed by a 5 °C per min ramp to 175 °C for 8 h.

8. Evaluation of Hardness Measuring Technique

Once the specimens had completed all thermal cycles (aluminum and titanium), two flats approximately 1 mm deep were machined from the specimens. After the Jominy end quench specimen is quenched, the hardness must be measured. The hardness scale generally used for steel is the Rockwell™ "C" scale (Diamond Braile Indenter, 150 kg load). In steel, hardnesses are taken every 1/16 in., measured from the quenched end. For this investigation, the Diamond pyramid hardness or Vickers hardness scale (1.5 kg load) was used. This hardness measuring technique allows the indentations to be spaced at much closer intervals (1/64 in.), enabling the observation of subtle trends in hardness, and shows improved repeatability. To ensure accurate positioning, a specially designed fixture was used. Because the hardness indentations are more closely spaced, the absolute position and relative interval must be known accurately. The existing Rockwell Equitron™ fixture was modified to allow positioning at much closer intervals (1/64 in.). A demonstration of the accuracy of the modified positioning device was accomplished by taking multiple Vickers hardness readings along a previously hardened Jominy end quench specimen. The absolute and relative positions of the hardness indentations were measured using a Nikon Toolmakers measuring microscope, with a calibrated tolerance of 0.001 in. While a slight periodic error was apparent, the average relative indentation spacing is 0.0156 in., with a standard deviation of 0.001 in. This is within the tolerance of the measuring microscope. Accurate positioning was therefore achieved.

9. Radial Heat Transfer and Effect on Hardness

A 7050 Jominy end quench test specimen previously heat treated was sliced at several distances from the quenched end. These slices were polished using the technique described above. Radial hardness traverses were taken at several distances from the quenched end to verify that excessive heat transfer along the sides of the cylinder did not occur. Results are shown in Fig. 3. The resulting radial hardness traverses are flat, confirming that heat transfer is along the cylinder axis, with little heat transfer occurring along the sides.

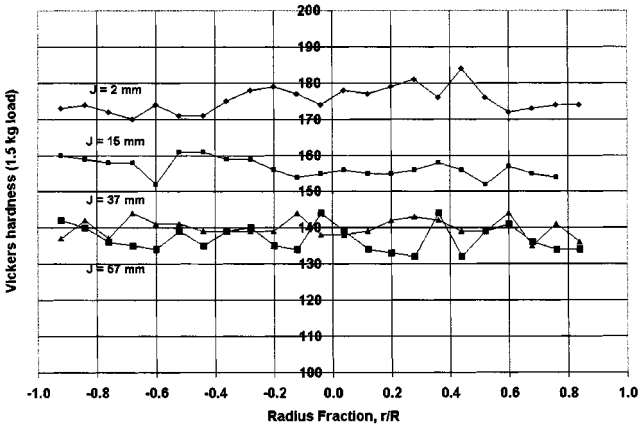

Fig. 3 Radial hardness traverse of an aluminum Jominy end quench specimen showing only axial heat transfer

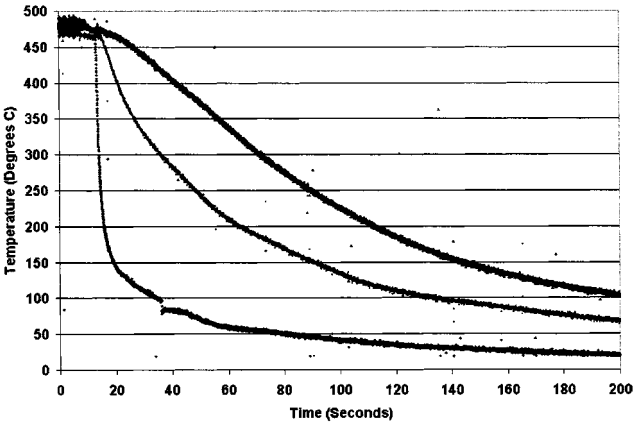

Fig. 4 Measure time-temperature curve of an aluminum Jominy end quench specimen

10. Verification of Cooling Rates

The test specimens were prepared previously by drilling small (1.5 mm) radial holes at 3.2, 38.1, and 76.2 mm from the quenched end of the aluminum Jominy specimens. These holes were drilled to a depth of 12 mm (the center of the specimen). Type K thermocouple wires (Special Limits of Error, 24 AWG) were inserted into the radial holes until intimate contact was made. Once the thermocouples or the thermocouples and the wire were inserted, the thermocouples were held in place using the high temperature fiberglass tape. All thermocouples were taken from the same roll and were previously calibrated.

The test specimens, with thermocouples attached, were inserted one at a time, into the middle of the furnace work

zone, near the furnace control thermocouple. The temperature readings of the thermocouples were monitored and allowed to reach the furnace temperature (approximately 25 min). The parts were allowed to soak for 45 min. The data acquisition unit was activated and allowed to collect steady-state temperature data. The data acquisition rate was 50 Hz.

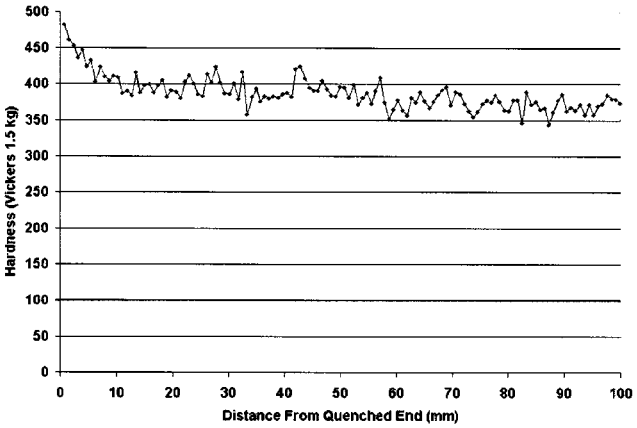

Fig. 5 Ti-6V-4Al Jominy end quench hardness profile

The resulting time-temperature cooling curves are presented in Fig. 4. The cooling rate at specific temperatures was determined by taking the time and temperature 25 °C above and below the desired temperature on the time-temperature cooling curves. These curves show that there is a progressive change in the cooling rate as the distance from the quenched end is increased.

11. Jominy End Quench Evaluation of Ti-6V-4Al, 7075, and 7050 Aluminum

In this section, several examples of the use of the Jominy end quench test in examining two nonferrous systems will be illustrated.

11.1 Titanium

A 72 mm round of Ti-6V-4Al was machined to conform to the Jominy end quench specimen dimensions. The specimen was solution heat treated in the â region and quenched in the Jominy fixture. Two flats were machined from the Jominy

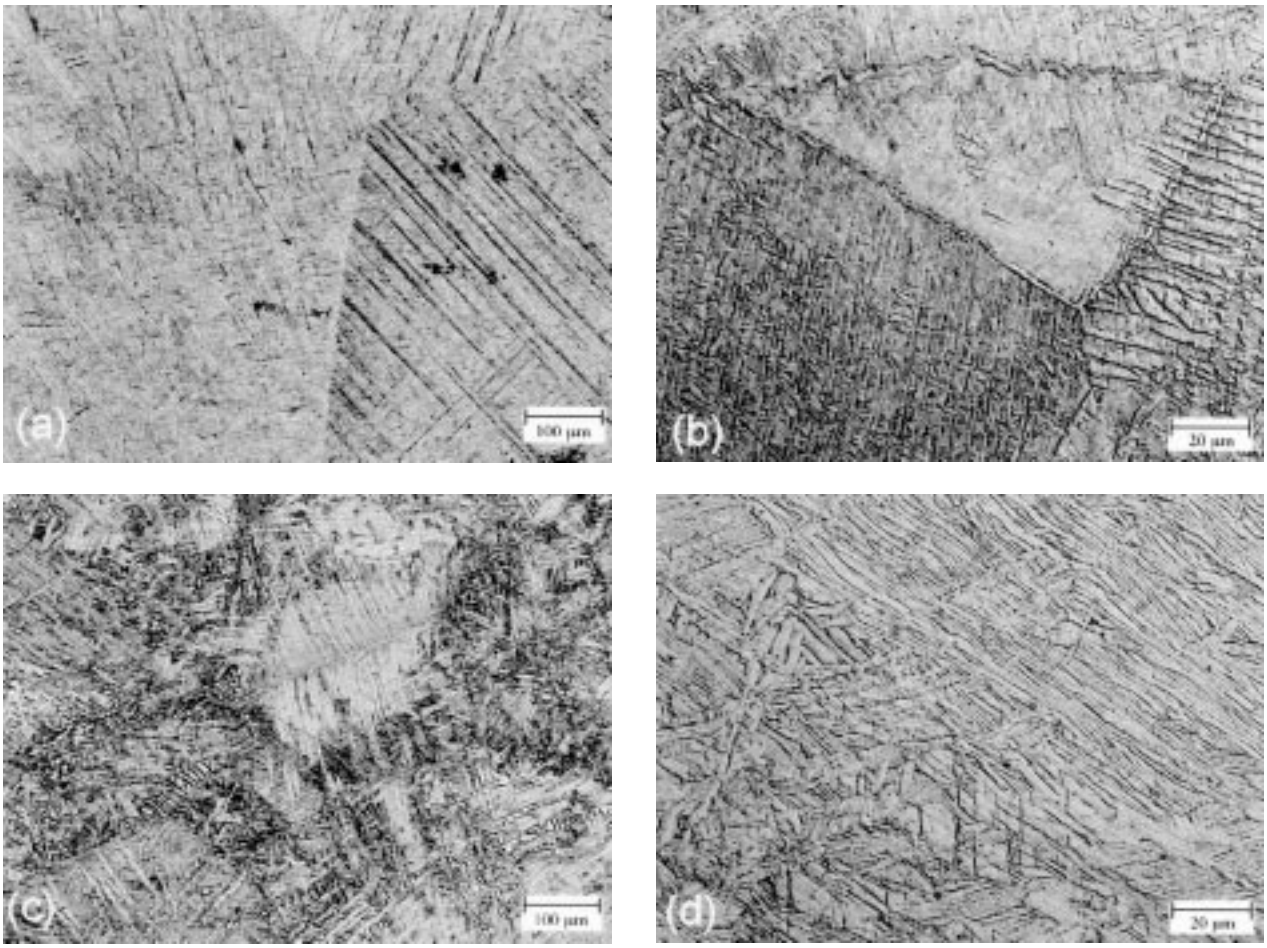

Fig. 6 Microstructure changes in Ti-6V-4Al as a function of quench rate and position on the JEQ bar: (**a**) $J = 2$ mm, (**b**) $J = 10$ mm, (**c**) $J = 50$ mm, and (**d**) $J = 100$ mm

specimen, and a hardness traverse was performed (Fig. 5). The results show that the hardenability of this alloy is low, with the region of highest hardness very shallow.

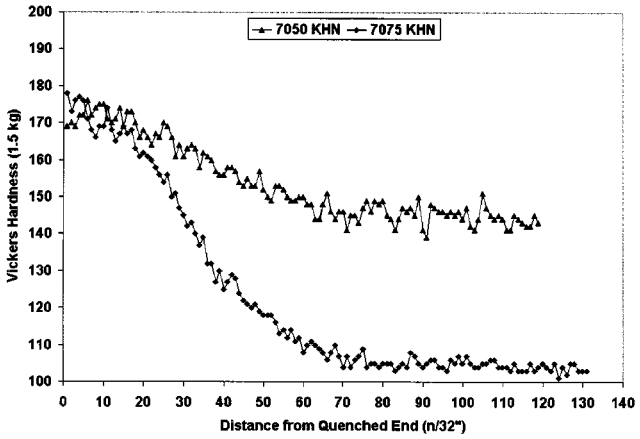

Fig. 7 Hardness profiles of 7075 and 7050 aluminum Jominy end quench specimens

Photomicrographs taken along the length of the titanium Jominy end quench specimen show a dramatic change in microstructures (Fig. 6). In the first several millimeters, the microstructure is predominately α with prior α grain boundaries. As the cooling rate slows, the microstructure becomes very complex, with evidence of primary α, Widmanstätten structure, and α at the prior α grain boundaries. Some acicular α is also present. Upon further cooling, the microstructure becomes entirely Widmanstätten structure. Cooling never became slow enough to show a completely equiaxed $\alpha + \alpha$ microstructure.

11.2 Aluminum

The resulting hardness and conductivity of the 7050 and 7075 Jominy end quench specimens are shown in Fig. 7. This shows that 7075 is much more quench sensitive than 7050. In addition, the inflection points on the hardness curves are nearly identical. The cause of similarity is not yet known.

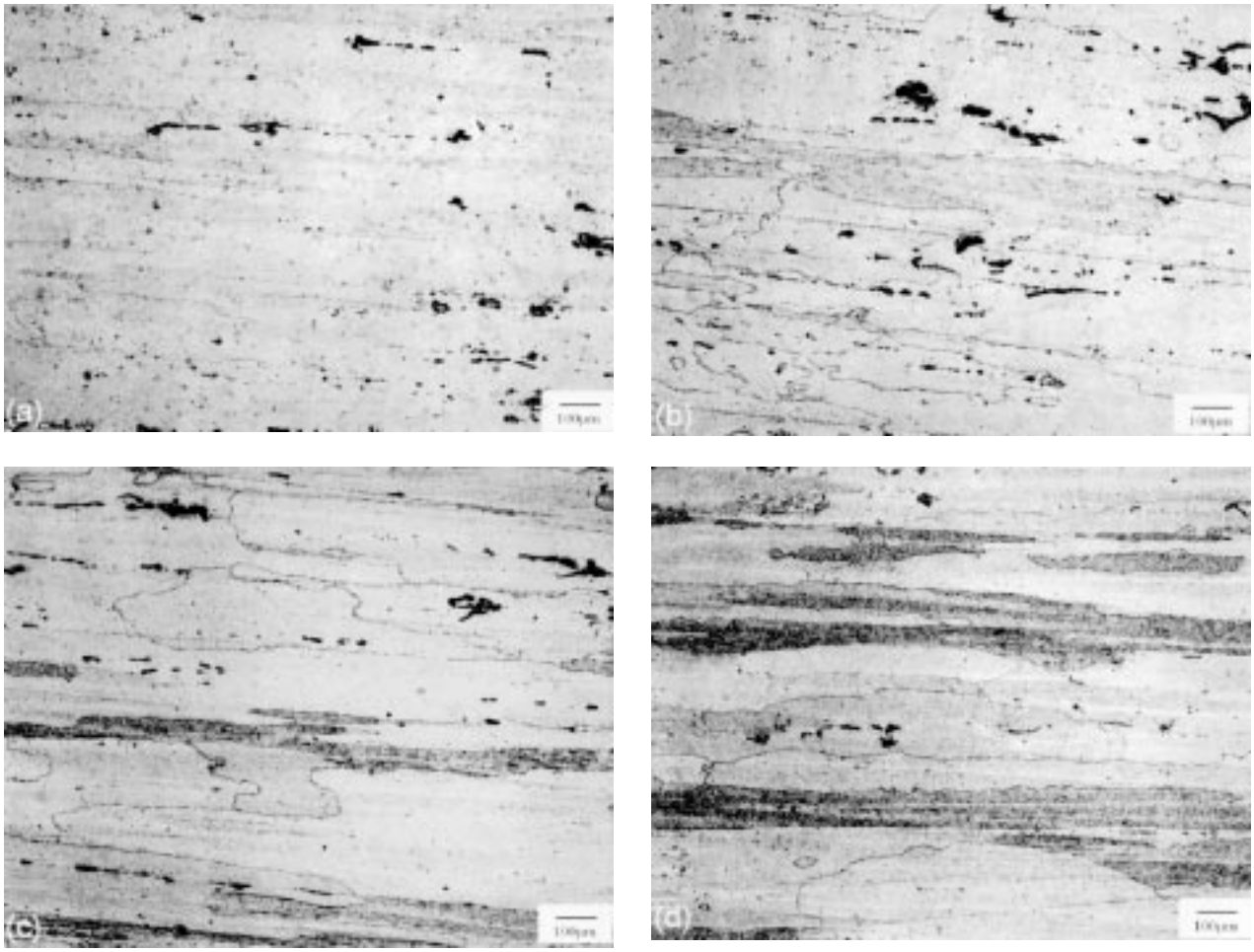

Fig. 8 Microstructure changes in 7050 aluminum as a function of quench rate and position on the JEQ bar: (**a**) $J = 2$ mm, (**b**) $J = 10$ mm, (**c**) $J = 50$ mm, and (**d**) $J = 100$ mm

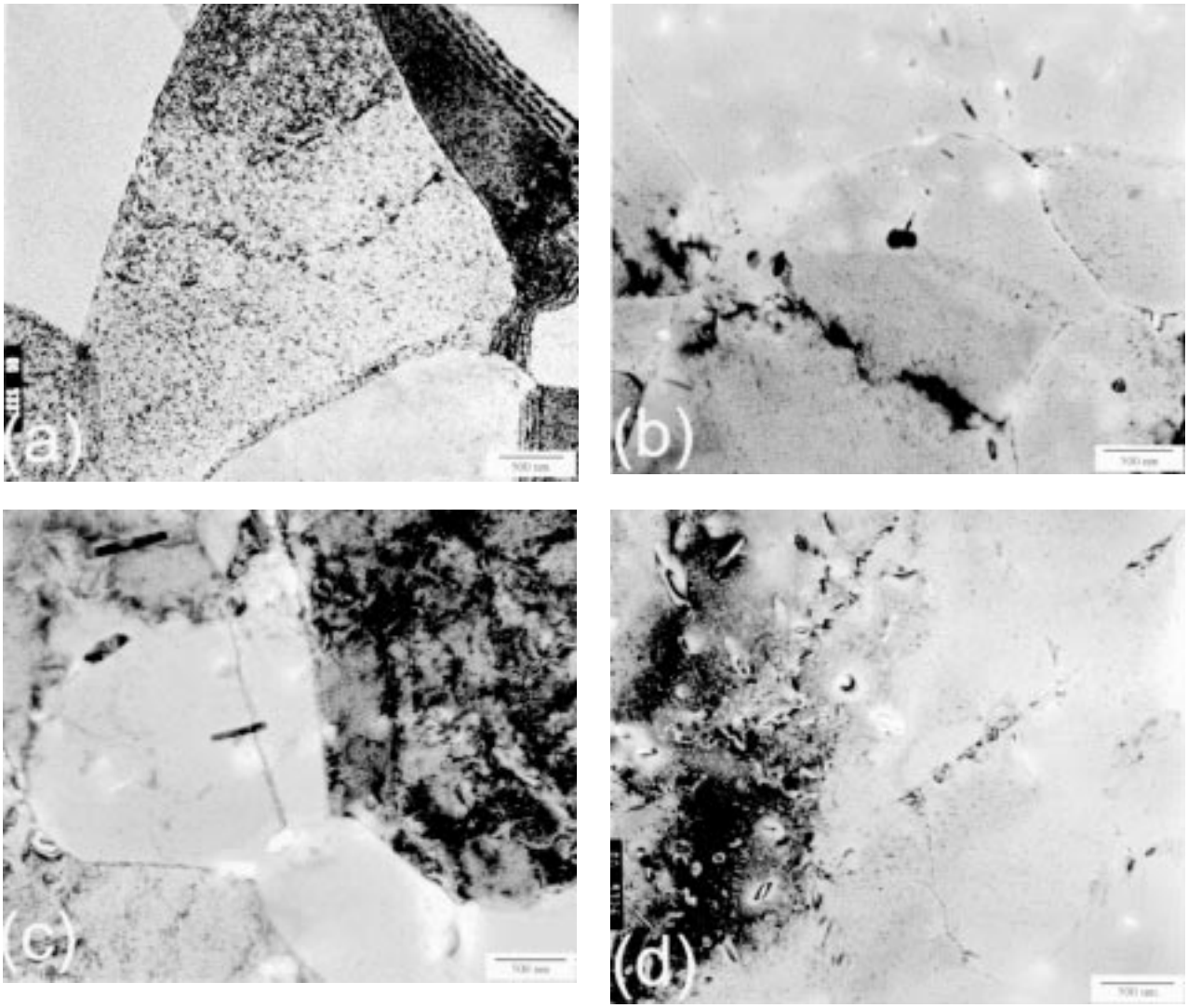

Fig. 9 TEM examination of changes in microstructure occurring in 7050 aluminum as a function of quench rate and position on the Jominy end quench bar: (**a**) $J = 7$ mm, (**b**) $J = 31$ mm, (**c**) $J = 56$ mm, and (**d**) $J = 79$ mm

12. Optical Examination of Aluminum Jominy End Quench Specimens

The microstructure was also examined optically to evaluate whether changes in microstructure could be distinguished as a function of cooling rate. The results of the microstructural examination of the 7050 and 7075 microstructure are shown in Fig. 8. At 10 mm from the quenched end, grain boundaries are outlined parallel to the rolling direction. Very little etching of the grain boundaries perpendicular to the rolling direction was observed. Some larger secondary precipitates are visible. As the cooling rate slows ($J = 25$ mm), darker grain boundaries are evident. Etching and precipitation appear to be occurring preferentially in some grains. Some grain boundaries perpendicular to the rolling direction are evident. At $J = 50$ mm, increased precipitation in the interior of the grains and at the grain boundaries is observed. Precipitation is still preferred in some grains more than others. More perpendicular grain boundaries are evident. In the final location ($J = 100$ mm), precipitation is much more uniform. Parallel and perpendicular grain boundaries are more darkly etched. The microstructure is typical of an overaged microstructure. These results indicate that initial precipitation occurs in some grains preferentially over others. This may be related to a preferred orientation of the precipitates.

13. TEM Examination of 7050 Jominy End Quench Specimens

Transmission electron microscopy 3 mm disks were prepared perpendicular to the rolling direction, by taking slices at specific distances from the quenched end. Specimens were punched from thin slices and mechanically ground and polished to approximately 125 μm thick. The 3 mm disks were then electropolished using 25% HN_{O3} in methanol at -20 °C. Voltage used

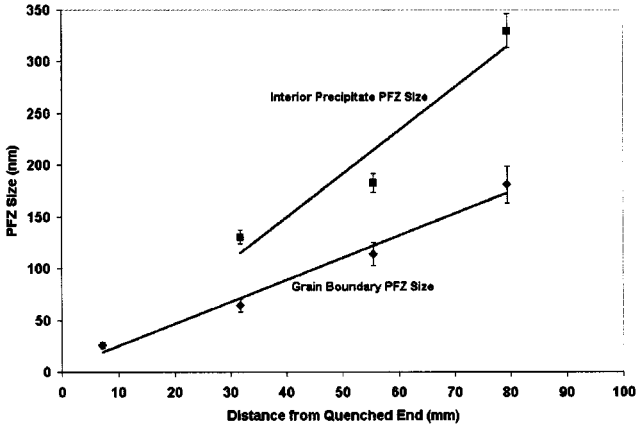

Fig. 10 PFZ width as a function of distance from the quenched precipitation could be followed as a function of cooling rate. Measurements of PFZ widths followed a linear relationship with the Jominy distance

was 14 V DC. The disks were then examined in a Philips EM430 at 300 kV.

Using bright-field conditions, images of four positions at varying distances from the quenched end were taken (Fig. 9). At a position close to the quenched end ($J = 7$ mm), the grains have a strong diffraction contrast. A mottled appearance is evident from the presence of strain contrast around the coherent or semicoherent precipitates. No large precipitates were found except at the grain boundaries. Evidence of serrated grain boundaries was found, probably from pinning. At slower cooling rates, larger and coarser precipitates from quenching occurred at the grain boundaries and at the interior of the grain. The lack of strain contrast indicates that the precipitates are now incoherent.

The complete width of the PFZ around the grain boundary and interior quenching precipitates was measured and plotted as a function of position from the quenched end (Fig. 10). The results show that the PFZ increases in size as a linear function of distance from the quenched end. The results demonstrate clearly the relationship of the PFZ to cooling rate. In addition, based on the results of the Jominy end quench, the width of the PFZ can now be predicted. This has great significance toward the prediction of properties as a function of heat treatment.

14. Conclusions

The Jominy end quench has been shown to produce reproducible and expected structures and properties in Ti-6Al-4V, AAl 7050, and Al 7075. There is no significant effect of radial heat transfer during the test, making it truly uniaxial heat flow. Vickers pryamidal hardness yields the best results, in terms of reproducibility, accuracy, and the ability to resolve differences over small distances. The cooling rates can be measured and correlated with cooling rates in various cross sections, allowing faster quenching studies to be performed for commercial heat treating.

The microstructural evolution in the aluminum alloys could be easily followed by optical microscopy and TEM. Matrix precipitation and grain boundary precipitation could be followed as a function of cooling rate. Measurements of PFZ widths followed a linear relationship with the Jominy distance.

The results show that the Jominy end quench test is a powerful tool to examine the effects of quench rate and heat treating parameters. The test is appropriate for many different nonferrous alloys, where the alloy has properties that depend on the quench rate. It is highly recommended for quenching studies in age hardened aluminum.

Acknowledgments

The authors thank Century Aluminumy, Ravenswood Facility, for funding this work.

References

1. W.E. Jominy and A.L. Boegehold: *ASM Trans.*, 1939, vol. 27 (12), p. 574.
2. "Jominy Test, Standard Method for End-Quench Test for Hardenability of Steel," ASTM A255, *Annual Book of ASTM Standards*, ASTM, Philadelphia, PA.
3. "Methods of Determining Hardenability of Steels," SAE J406c, *Annual SAE Handbook*, SAE, Warrendale, PA.
4. W.E. Jominy: *ASM Trans.*, 1939, vol. 27 (12), p. 1072.
5. V. Hergat: *Traitement Thremique*, 1981, vol. 153, p. 49.
6. G.T. Brown: in *Hardenability Concepts with Applications to Steel*, D.V. Doane and J.S. Kirkaldy, eds., AIME, Warrendale, PA, 1978, p. 273.
7. A.K. Sheikh: *Proc. 3rd Int. Symp. on Advanced Materials*, 1993, TMS, p. 696.
8. J.G. Kura and C.H. Lorig: "Correlation of Cooling Velocity of the Standard Jominy Hardenability Test with the Cooling Velocity within the Cross-Section of Plates," Battelle Memorial Institute Report S-547, Battelle, Columbus, OH, June 2, 1942.
9. J.G. Kura and C.H. Lorig: "Correlation of Cooling Velocity of the Standard Jominy Hardenability Test with the Cooling Velocity within the Cross-Section of Plates," Battelle Memorial Institute Report S-547, Columbus, OH, July 23, 1942.
10. T. Toda: *J. Jpn. Inst. Met.*, 1965, vol. 29, p. 237.
11. P.J. Postans: "The Use of Jominy End Quench to Assess the Hardenability of Higher Strength Titanium Alloys," *DCAF 070028 Rolls Royce, Oct. 1*, London, U.K., *1983*.
12. B.M. Loring, W.H. Baer, and G.M. Carlton: *Trans. Am. Inst. Min., Met. Eng.*, 1948, vol. 175, p. 401.
13. W.G.J. 'tHart, H.J. Kolkman, and L. Schra: "The Jominy End-Quench Test for the Investigation of Corrosion Properties and Microstructure of High Strength Aluminum," NLR Tr 80102U, National Aerospace Laboratory, NLR, Netherlands, 1980.
14. W.G.J. 'tHart, H.J. Kolkman, and L. Schra: "Effect of Cooling Rate on Corrosion Properties and Microstructure of High Strength Aluminum Alloys," NLR TR 82105 U, National Aerospace Laboratory, NLR, Netherlands, 1982.
15. D. Hecker: *HTM*, 1975, vol. 30, p. 268.
16. H. Bomas: *HTM*, 1975, vol. 30, p. 274.
17. W.E. Arthur, R. Becker, and M.E. Karabin: *Proc. Int. Heat Treating Conf.—Equipment Processing, Rosemont, IL, May 18–20, 1994.*
18. R. Becker, M.E. Karabin, and J.C. Liu: Comput. Mater. Modeling - ASME, 1994, vol. 294, p. 287.